JAST (Journal of Animal Science and Technology) TITLE PAGE

ARTICLE INFORMATION	Fill in information in each box below
Article Type	Research article
Article Title (within 20 words without abbreviations)	Long noncoding RNA network for lncRNA-mRNA interactions throughout swine estrous cycle reveals developmental and hormonal regulations in reproductive tissues.
Running Title (within 10 words)	Long noncoding RNA analysis throughout swine estrous cycle
Author	Yoon-Been Park[1], Chiwoong Lim[1], Byeonghwi Lim[1] and Jun-Mo Kim[1]
Affiliation	Functional Genomics & Bioinformatics Laboratory, Department of Animal Science and Technology, Chung-Ang University, Anseong, Gyeonggi-do 17546, Republic of Korea
ORCID (for more information, please visit https://orcid.org)	Yoon-Been Park: 0000-0002-3557-785X Chiwoong Lim: 0000-0002-6272-4464 Byeonghwi Lim: 0000-0001-8489-0044 Jun-Mo Kim: 0000-0002-6934-398X
Competing interests	No potential conflict of interest relevant to this article was reported
Funding sources State funding sources (grants, funding sources, equipment, and supplies). Include name and number of grant if available.	
Acknowledgements	
Availability of data and material	
Authors' contributions Please specify the authors' role using this form.	Conceptualization: Yoon-Been Park and Jun-Mo Kim. Data curation: Jun-Mo Kim. Formal analysis: Yoon-Been Park and Byeonghwi Lim. Methodology: Yoon-Been Park and Chiwoong Lim.

	Software: Yoon-Been Park.
	Investigation: Chiwoong Lim and Byeonghwi Lim.
	Writing - original draft: Yoon-Been Park.
	Writing - review & editing: Jun-Mo Kim and Yoon-Been Park.
Ethics approval and consent to participate	This article does not require IRB/IACUC approval because there are no human and animal experiments.

CORRESPONDING AUTHOR CONTACT INFORMATION

For the corresponding author (responsible for correspondence, proofreading, and reprints)	Fill in information in each box below
First name, middle initial, last name	Jun-Mo Kim
Email address – this is where your proofs will be sent	junmokim@cau.ac.kr
Secondary Email address	
Address	Functional Genomics & Bioinformatics Laboratory, Department of Animal Science and Technology, Chung-Ang University, Anseong, Gyeonggi-do 17546, Republic of Korea
Cell phone number	+82-10-4026-5644
Office phone number	+82-31-670-3263
Fax number	+82-31-675-3108

Abstract

The mechanism of estrous cycles of pigs should be explored because their reproductive traits are useful for manipulating productivity and solving problems such as infertility. These estrous cycles should be elucidated to understand the complex interactions between various reproductive tissues (including the ovary, oviduct, and endometrium) and the complex range of hormone secretions during estrous cycles. Long non-coding RNAs (lncRNAs) regulate target genes at transcriptional, post-transcriptional, and post-translational regulation levels in various species. However, unlike mRNAs, lncRNAs in pigs have not been sufficiently annotated, and understanding the protein level of coding genes has limitations in determining the mechanism of the reproductive traits of porcine. In this study, the lncRNAs of the porcine ovary, oviduct, and endometrium were investigated on days 0, 3, 6, 9, 12, 15, and 18 of the estrous cycle. In addition, the characteristics and functions of the identified lncRNAs were explored. 19,021 novel lncRNA transcripts were selected, and the comparison of the characteristics of the newly identified lncRNA and mRNA showed that similar to those of previous studies. Four lncRNA networks were chosen through network analysis. The *cis*-acting genes of lncRNAs included in each network were identified, and expression patterns were compared. The main lncRNAs (XLOC_021792, XLOC_017111, ENSSSCG00000050977, XLOC_000342, ENSSSCG00000050380, ENSSSCG00000045111, XLOC_008338, XLOC_004128, and ENSSSCG00000040267) were determined from the network by considering the *cis*-acting genes. Specific novel lncRNAs were discovered in the reproductive tissues during the swine estrous cycle, and their time-serial expression dynamics were confirmed. As the main lncRNAs are involved in the development of each reproductive tissue and hormone action, they can be utilized as potential biomarkers to help improve and develop the reproductive traits of pigs.

Introduction

The porcine reproductive trait is one of the most important factors in the competitiveness and efficiency of the pig industry, and the reproductive trait of female pigs in particular is directly related to porcine reproductive efficiency [1, 2]. The reproductive efficiency in female pigs remarkably affects the litter size, fertility, and hormonal metabolism of pigs [3-5]. Various hormones interacting with one another according to the estrous cycle in turn influence reproductive efficiency [6-8]. Since hormones are secreted and regulated by several reproductive tissues during the estrous cycle, porcine reproductive efficiency is closely associated with molecular mechanisms involved in pig reproductive tissues [9]. Among these reproductive tissues, the ovaries are important because they are a source of reproductive hormones and follicles [10]. They also respond to vital hormones secreted by other organs, especially the pituitary gland, which produces major steroid hormones (estradiol [E4] and progesterone [P2]) and peptide growth factors implicated in the functioning of the ovaries [9, 11]. In addition, the oviduct carries follicles from the ovary to the uterus, and its metabolites are affected by ovarian hormones such as E4 and P2 [12, 13]. The follicles that ovulate from the ovary move through the oviduct into the uterus. The endometrium is an inner wall of the uterus that prepares for implantation through morphological and functional changes; it also communicates with the ovary through the secretion of prostaglandin F2α (PGF2α) [6, 14, 15]. Despite relevant studies, the interaction and hormone control mechanisms of reproductive tissues according to the estrous cycle remain difficult and complex. Previous studies showed that a co-expression network can be integrated using whole transcriptomes in each tissue [16, 17] and multiple reproductive tissues [6, 16, 17], but the synchronized interaction of pig reproductive tissues according to the estrous cycle is still insufficient because it is too complicated to be identified only via analysis at the mRNA level.

49   With the development of next generation sequencing (NGS) technology, noncoding

50   RNAs, which occupy much more areas but do not encode proteins, can be examined [18].

51   Among noncoding RNAs, long noncoding RNAs (lncRNAs) with a length of 200 bp or more

52   have lower gene expression levels than protein-coding genes, but genes are regulated through

53   transcriptive regulation, post-transcriptive regulation, and RNA interference [19-22]. Most

54   lncRNAs are located in the chromatin and can interact with proteins to promote or inhibit DNA

55   activity in the target DNA region [23]. Therefore, lncRNAs play an important role in genome

56   studies, such as those focusing on mRNA regulation; their characterization in the animal

57   genome can be a key to bridging the gap between genotypes and phenotypes [24]. In addition,

58   the importance of lncRNA is being studied in the fields of infectious diseases, immunity, and

59   pathology; it is considered an important factor in stress response and development regulation

60   in animals [7, 25, 26]. Thus, lncRNAs have crucial roles in tissue- and species-specific

61   regulation of biological processes in various species and tissues [27-30]. Currently, studies

62   involving lncRNA analysis have been conducted in pig reproductive tissues, but only a few

63   have explored a single tissue (ovary, oviduct, endometrium) [7, 14, 31].

64   Multi-omics analyses have been conducted to obtain complex biological processes

65   holistically [32, 33], and lncRNAs have been considered as a factor for such integrated analysis

66   [34]. The limitations of mRNA-level analysis can be complemented by analyzing the

67   mechanism by which lncRNA manipulates mRNA. In this study, candidate novel lncRNAs

68   were determined, and novel and known lncRNA expression patterns were explored via RNA-

69   seq in three reproductive tissues (ovary, oviduct, and endometrium) throughout the porcine

70   estrous cycle. Significant lncRNA–mRNA pairs were determined to identify tissue- and period-

71   specific lncRNA and mRNA expression and to construct the main lncRNA networks. This

72   study was conducted to confirm the characteristics of lncRNAs according to estrous cycle and

73   reproductive tissues and identify the relationship between lncRNAs and mRNAs by verifying

5

74 the regulatory mechanisms of lncRNAs to mRNAs.

Methods

Ethics, Sampling, and Sequencing

All animal experimental procedures were approved by the Institutional Animal Care and Use Committee of the National Institute of Animal Science, Republic of Korea (No. 2015-137) and conducted following the Guide for Care and Use of Animals in Research.

Twenty-one crossbred (Landrace × Yorkshire) gilts (age = 6–8 months; weight = 100–120 kg) that underwent at least two normal estrous cycles were used in this study. Three reproductive tissues (ovary, oviduct, and endometrium) of the gilts were collected for sequencing (Figure 1) on days 0 (designated as the first day of detection of estrous behavior; D00), 3 (D03), 6 (D06), 9 (D09), 12 (D12), 15 (D15), and 18 (D18).

Total RNA was extracted from all reproductive tissues by using TRIzol reagent (Invitrogen, Life Technology, Carlsbad, CA, USA). RNA integrity was evaluated through electrophoresis in 1% agarose gel, and RNA quantity was verified using a NanoDrop ND-1000 spectrophotometer (NanoDrop Technologies, Wilmington, DE, USA). Individual libraries were prepared using an Illumina TruSeq RNA sample preparation kit, and sequencing was performed using cDNA libraries constructed via the 100-base pair (bp) pair-end method in llumina HiSeq 2000. All raw RNA-seq data were deposited at the NCBI Gene Expression Omnibus (https://www.ncbi.nlm.nih.gov/geo/) under the accession number GSE108570. Relevant information was described in detail in our previous study [6, 16].

Computational identification of lncRNAs

FastQC software (v.0.11.8) was used to check the quality of raw reads of each sample. For quality control, the reads were processed using Trimmomatic software (v0.39), which removes adaptors and low-quality reads. Hisat2 (v2.1.0) was utilized to map clean reads to the

100   reference genome (Sus scrofa Sscrofa 11.1.99, GCA_000003025.6) of the Ensembl genome

101   browser (http://www.ensembl.org/Sus_scrofa/) as a basis for vsubsequent StringTie application.

102   Samtools (v1.9) was also used to sort the reads mapped in accordance with the criteria for

103   subsequent StringTie application. The transcript assembly of each sample sorted by the

104   StringTie (v2.1.3b) program was prepared using the reference annotation file (Sus scrofa

105   Sscrofa 11.1.99). The GTF files of each obtained sample were merged and compared through

106   the gffcompare program (v 0.11.6) and converted through the gffread (v 0.11.8). For the

107   screening of potential novel lncRNAs, those with transcript lengths longer than 200 bp and

108   those with class codes "I", "j", "o", "u", and "x" were selected. TransDecoder (v5.5.0) was

109   used to determine the transcripts with an open reading frame (ORF) length of less than 300 bp.

110   Furthermore, CPC2 (Coding Potential Calculator2), PLEK (predictor of long non-coding

111   RNAs and messenger RNAs based on an improved k-mer scheme) v1.2, CPAT (RNA coding

112   potential assessment tool) v1.2.4, and CNCI (Coding-Non-Coding Index) were used to predict

113   the coding potential of the remaining transcripts. Transcripts with a high probability of non-

114   coding were selected using information from the PFAM (v33.0, The protein families) and

115   RFAM (v14.2 The RNA families) databases. The HMMER program (v3.3) was used to filter

116   the known protein family domain, and the internal program (v1.1.2) was used to filter

117   housekeeping RNAs. Transcripts presumed to be potential lncRNAs were removed in only 1

118   out of 68 samples (ovary, oviduct, endometrium). The processes used to identify novel

119   lncRNAs are illustrated in Figure 2A.

120

121   ***Characteristics of putative lncRNAs***

122   Various genomic characteristics were identified to confirm the specific properties of the

123   newly obtained lncRNA. The number of exons, transcript length, and genomic location were

124   determined through a final combined GTF file (Figure 2A). Since tissue specificity is a notable

feature of lncRNA, the tissue specificity index (TSI) of lncRNA was calculated. The lncRNAs used included the novel lncRNAs and known lncRNAs. The TSI is calculated as follows:

$$TSI = \frac{\sum_{i=1}^{N}(1-x_i)}{N-1},$$

where N is the number of tissues, and x_i is the fragment per kilobase of exon per million mapped fragments (FPKM) value of lncRNA/mRNA x in tissue i normalized by the maximum value of FPKM [35].

Overall expression levels of lncRNA and mRNA genes

The expression patterns were obtained to determine tissue-specific and timepoint-specific lncRNAs and mRNAs according to the estrous cycle. The trimmed mean of M (TMM) value was used to normalize raw counts and estimate the expression levels of lncRNAs and mRNAs. Differential expression analyses were performed at each time point (D03, D06, D09, D12, D15, and D18) and compared with those at D00 for each tissue (ovary, oviduct, and endometrium) by using the R package (edge R 3.32.1); an absolute log2 fold-change (FC) of ≥1 and false discovery rate (FDR) of <0.05 were used as cutoff criteria for differentially expressed (DE) lncRNAs and mRNAs. A multidimensional scaling (MDS) plot and a volcano plot of DE lncRNAs and mRNAs were drawn by ggplot2 and limma function of the R package.

Network construction of lncRNAs

Network analysis was conducted via weighted gene co-expression network analysis (WGCNA) package in R to examine their correlation between lncRNAs and phenotypes (tissue and time specific according to the estrous cycle and hormonal changes). Hormone-related traits consisting of steroid hormones (follicle-stimulating hormone [FSH], luteinizing hormone [LH], P4, E2, inhibin) that play important roles in the estrous cycle [11]. Hormone data were

149   measured from blood samples at seven time points (D00, D03, 06, D09, D12, D15, and D18)

150   over the estrous cycle, and detailed methods and explanations are described in the paper [36].

151   The content of these hormonal traits is summarized in Table S1. Correlations were calculated

152   on the basis of co-expression, and the module (network) with high correlation was constructed

153   using the $\log_2$TMM value of lncRNA. In the case of hormone traits, the data corresponding to

154   each estrous cycle at seven time points were analyzed for correlation and expressed as a

155   correlation coefficient. Among the modules, three tissue-specific modules (ovary, oviduct,

156   endometrium specific) and one hormone-specific module were selected. Network visualization

157   was performed using the Cytoscape (v3.8.2) software.

158

159   ***Cis-nearby targeted DEmRNAs of lncRNAs***

160   *Cis*-acting genes were confirmed from the main lncRNAs in four networks. *Cis*-

161   regulatory elements or *cis*-regulatory modules are noncoding DNA regions that regulate the

162   transcription of neighboring genes [37]. In *cis*, lncRNA regulates nearby sequences in the

163   genome, and various related results confirmed that such lncRNAs are found within 100 kb of

164   transcriptional regulation-related coding genes [37]. Therefore, coding genes were searched

165   within 100 kb upstream and downstream of the main lncRNA because the *cis*-activity of

166   lncRNA is related to interaction with adjacent target genes [35, 38]. The expression patterns of

167   lncRNAs and their *cis*-acting genes of each network in tissues and time point were confirmed

168   using Multi Experiment Viewer (MeV v4.9.0) by the k-means clustering algorithm. The

169   number of the main lncRNAs and main DE lncRNAs was shown as a circos plot; their *cis*-

170   acting genes and DE *cis*-acting genes were determined using the circa program (v1.2.1).

171

172   ***Functional analyses***

173   Database for annotation, visualization, and integrated discovery (DAVID) 2021 was used

174   to annotate the gene ontology (GO) term and the Kyoto Encyclopedia of Genes and Genomes

175   (KEGG) pathways by using the DE *cis*-acting gene of lncRNAs in the four networks. The

176   ClueGo (v2.5.7) plugin of Cytoscape (v3.8.2) was used to visualize GO terms and KEGG

177   pathways. A pie chart was drawn for the path that met the threshold value of $p < 0.05$, and the

178   KEGG pathways were visualized as a bar graph with $-\log_{10} P$-value and fold enrichment.

Results

Data processing

The RNA-seq reads were generated at seven time points during the estrous cycle in three tissues (ovary, oviduct, and endometrium; Figure 1) [6]. In 67 tissue samples (from three tissues), 1.3 billion sequence reads were produced with an average of 19.5 million per sample (Table S2). The average number of the clean reads after trimming was 1.1 billion sequence reads. The average unique mapping rate (93.93%) and the average overall mapping rate (97.81%) were determined. The MDS results based on transcriptomes (lncRNA and mRNA) showed that the clusters clearly separated for each tissue were common in lncRNAs and mRNAs (Figure S1).

Identification of novel lncRNA

After 627,357 transcripts were obtained through assembly and merging, 626,016 transcripts remained except for those less than 200 bp in length. After the class codes (i, j, o, u, x) of the candidate lncRNA were extracted, 393,933 transcripts remained; of these transcripts, 94,727 had an ORF length of less than 300 bp. Then, 70,929 transcripts were derived using four coding potential assessment tools and two databases; finally, 19,021 novel lncRNA transcripts, excluding the transcripts identified in only one sample (Figure 2A, Table S3), were obtained.

Characteristics of lncRNA

Various types of information about the predicted lncRNA were first investigated and then compared with those of mRNA to determine the genomic characteristics of the acquired novel lncRNA. The average exon number of novel lncRNAs was 2.4, the known lncRNAs was 2.8,

204 and the protein-coding mRNA was 12.3, indicating that lncRNAs tended to be less than

205 mRNAs (Figure 2B). The mean transcript length of the novel ncRNA was about 18,763 bp, the

206 known lncRNA was about 22,846 bp, and the protein-coding mRNA was about 56,276 bp. The

207 transcript length also showed that lncRNAs tend to be shorter than mRNAs (Figure 2C), which

208 were consistent with previous studies [39, 40]. In addition, the transcript location of the novel

209 lncRNA was classified as follows: 31.3% of intergenic regions that did not overlap with the

210 protein-coding gene, 17.3% of intronic, 28.5% of sense exonic, 17.8% of antisense exonic, and

211 5.1% bidirectional (Figure 2D). Finally, the TSI was calculated to determine the tissue

212 specificity of lncRNAs. Similar to previous results [29], the average TSI (0.73) of lncRNAs

213 was higher than the average TSI (0.64) of mRNAs (Figure 2E).

214

215 ***Differential expression of lncRNA and mRNA***

216 The differential expression levels of lncRNAs and mRNAs in each of the three

217 reproductive tissues (ovary, oviduct, and endometrium) were investigated at six time points

218 (D03, D06, D09, D12, D15, and D18) based on the estrous cycle D00 (Figure 1). The patterns

219 of changes in the upregulated and downregulated expression levels of lncRNA and mRNA for

220 each tissue were similar (Figure S2). The number of DE transcripts in the ovary gradually

221 decreased until D18 after many differential expression levels were observed on D06 and D09.

222 The number of DE transcripts in the endometrium also increased until D09 and then gradually

223 decreased. In the oviduct, DE transcripts increased until D12 and decreased thereafter; the

224 smallest number of DE transcripts was also found in the oviduct (Figure S3). In addition, the

225 number of overlapping DE lncRNAs in the three tissues at each time point was relatively

226 smaller than that of DE mRNA (Figure S4). The list and significant values of all DE lncRNAs

227 and mRNAs are summarized in Table S4.

228

Co-expression network of lncRNA

Six modules (networks) of lncRNAs that correlated with hormones, reproductive tissues, and time points were calculated (Figure S5). Among them, four modules (blue, green, red, and yellow) were set to represent high significance with traits. Blue, green, and red modules were highly correlated in each of the three tissues (ovary, oviduct, and endometrium), and the yellow module was correlated with changes in each hormone (Figure 3A). The blue, green, red, and yellow modules had 3,243, 2,725, 2,682, and 24 lncRNAs, respectively, and four co-expression networks were generated using the WGCNA from these four modules. The blue network, which showed an ovary tissue-specific correlation, consisted of 130 nodes (lncRNAs) and 234 edges (interactions); it also had the largest number of nodes (Figure 3B). The green network, which showed oviduct tissue-specific correlation, comprised 45 nodes and 181 edges (Figure 3C). The red network, which exhibited endometrium tissue-specific correlation, consisted of 93 nodes 265 edges (Figure 3D). The yellow network, which indicated the correlation with hormones, had 20 nodes 30 edges (Figure 3E). Among the lncRNAs constituting the network, DE lncRNA had the highest number of 70 in the blue network and the smallest number of 8 in the green network; furthermore, 27 and 16 DE lncRNAs were found in the red and yellow networks, respectively.

Cis-acting gene profiling based on the main lncRNA

The *cis*-acting gene of each lncRNA was searched to identify the coding genes regulated by the main lncRNAs in the network [37]. These lncRNAs and *cis*-acting genes were distributed in all chromosomes except chromosome 7, and relatively many *cis*-acting genes were found in the blue and red networks in proportion to the number of lncRNAs (Figure 4). Furthermore, 240 *cis*-acting genes were identified from 130 lncRNAs in the blue network, 152 *cis*-acting genes were identified from 45 lncRNAs in the green network, 262 *cis*-acting genes

254 were identified from 93 lncRNAs in the red network, and 48 *cis*-acting genes were identified

255 from 20 lncRNAs in the yellow network, which were visualized in the outer layer. Among the

256 *cis*-acting genes searched in this way, 105 in blue networks, 56 in green networks, 112 in red

257 networks, and 18 in yellow networks were differentially expressed, and they were shown in the

258 middle layer of the *cis*-acting gene category. Among them, the DE *cis*-acting genes of DE

259 lncRNAs in each network were found in the inner layer, with 48 blue networks, 13 green

260 networks, 31 red networks, and 14 yellow networks. The *cis* interactions between them and the

261 main DElncRNA were visualized as a line in the innermost circle. A list of lncRNAs and *cis*-

262 acting genes is presented in Table S5.

263

264 ***Functional Annotations***

265   Naturally, lncRNAs with a *cis*-acting mechanism have low expression levels, and they

266 have the potential to regulate mRNAs even with such a low expression [37]. Therefore,

267 functional analysis was performed with the genes in the middle layer of the *cis*-acting gene

268 category in Figure 4. First, the expression patterns of DE *cis*-acting genes and lncRNAs

269 interacting with one another were compared. In each of the three tissue-specific networks, two

270 expression patterns were determined: a cluster in which the expression patterns of the two

271 groups of genes were directly proportional and another cluster in which the expression patterns

272 of the two groups of genes were inversely proportional to the ovarian tissue (Figure S6A-C).

273 In addition, in the hormone-specific network, the two gene groups were distinguished with two

274 expression patterns: a cluster that was directly proportional to the whole tissue and a cluster

275 that was inversely proportional to the whole tissue (Figure S6D).

276   From the DE *cis*-acting genes corresponding to the blue module network, the KEGG

277 pathways (neuroactive ligand-receptor interaction, ubiquitin mediated proteolysis, etc.) and BP

278 terms (regulation of ion transmembrane transport, protein polyubiquitination, etc.) were

279 enriched (Figure 5A). From the DE *cis*-acting genes corresponding to the green module

280 network, the KEGG pathways (tight junction, thyroid hormone synthesis, etc.) and BP terms

281 (positive regulation of MAP kinase activity, positive regulation of cell migration, epithelial cell

282 morphogenesis, toxin transport, etc.) were enriched (Figure 5B). From the DE*cis*-acting genes

283 corresponding to the red module network, the KEGG pathway (metabolic pathways) and BP

284 terms (vitamin A metabolic process, retinoic acid biosynthesis, N-terminal protein amino acid

285 acetylation, T cell costimulation, etc.) were enriched (Figure 5C). From the DE *cis*-acting genes

286 corresponding to the yellow module network, BP terms (skin development, cellular-modified

287 amnio acid catabolic process, organic acid catabolic process, etc.) were enriched (Figure 5D).

288 The detailed information on enriched genes and their significant values are summarized in

289 Table S6.

290   *FSHR*, *KCND2*, and *KCNQ5* were the main *cis*-acing genes involved in functional

291 analysis of the lncRNAs of the blue module network, and the lncRNAs with a *cis*-acting

292 relationship were identified to be XLOC_021792, XLOC_017111, ENSSSCG00000050977,

293 XLOC_000342, and ENSSSCG00000050380 (Figure 6A). The main *cis*-acing genes involved

294 in the functional analysis of the genes of the green module network were *ERBB2* and *DNM1*;

295 ENSSSCG00000045111, XLOC_003255, XLOC_003256, and XLOC_003257 were the

296 lncRNAs having a *cis*-acting relationship with them (Figure 6B). *RBP1*, *NMNAT3*, and *DLX5*

297 were the main *cis*-acing genes involved in the functional analysis of the genes of the red module

298 network, and XLOC_008338, XLOC_037548, and ENSSSCG00000051124 were the lncRNAs

299 showing a *cis*-acting relationship with them (Figure 6C). *KLF6*, *KLF11*, and *MYBL2* were the

300 main *cis*-acing genes involved in the functional analysis of the genes of the yellow module

301 network; XLOC_004128, ENSSSCG00000040267, and XLOC_016616 were the lncRNAs

302 having a *cis*-acting relationship with them (Figure 6D).

Discussion

Dynamic changes in lncRNAs during the estrous cycle

Swine reproductive tissues undergo various tissue-integrated and tissue-specific changes during the estrous cycle. During the proestrus period (D16-D21), FSH is secreted by GnRH in preparation for estrus, and estrogen secretion increases as the follicle matures for ovulation [9]. At this time, E2, an estrogen steroid hormone, thickens the lining of the uterus to create an environment where a follicle can be implanted when the follicle is fertilized [41]. After the peak of E2 and FSH secretion in the estrus period (D00–D03), fully mature follicles become ovulated [9]. In the metestrus period (D04–D06), luteinization begins, P4 secretion begins, and the follicle from the oviduct is released [17]. In diestrus (D07–D15), which is the longest phase of the estrus cycle, the corpus luteum continues to develop in the ovary, and P4 secretion increases continuously [9]. P4 helps keep the endometrium fertile and stimulates PGF2α secretion by the endometrium [42-44]. If pregnancy is not achieved until approximately D15, PGF2α is secreted from the endometrium to the ovary, and the corpus luteum is degenerated to reduce P4 secretion, contract the uterus, and return to the proestrus state [45, 46]. With these changes, the mRNA expression undergoes tissue-integrated and tissue-specific changes during the estrous cycle [6]. The lncRNA expression also changes, and its expression pattern is similar to that of mRNA (Figure S2, S3). This finding suggests that mRNAs and lncRNAs are involved in the changes in three reproductive tissues during the estrous cycle. In this study, WGCNA analysis was performed to determine the correlation between these lncRNAs. Among the modules constructed through lncRNA co-expression analysis, the tissue-specific lncRNAs of three reproductive tissues during the estrous cycle were investigated using three modules, and tissue-integrated lncRNAs were examined by identifying hormonal changes in the three tissues

327   using one module. These generated modules revealed the existence of lncRNAs specifically

328   regulated by tissue or hormonal changes.

329

330   ***Development of each tissue by the main lncRNA and cis-acting gene***

331   First, the tissue-specific lncRNAs of the ovary were obtained from the network

332   constructed through the blue module (Figure 3B). BP terms and KEGG pathway enrichment

333   analyses were performed to reveal the association between the molecular function of the

334   corresponding DE *cis*-acting gene of lncRNAs and the estrous cycle. Numerous main terms

335   essential for ovarian development and function were identified (Figure 5A).

336   Among the lncRNA and *cis*-acting gene pairs involved in these functions, five pairs had

337   significant expression patterns and correlations (Figure 6A). Previous studies confirmed that

338   the neuroactive ligand-receptor interaction pathway may play an important role in follicle

339   production and ovarian function regulation in poultry and fish; it may also influence steroid

340   hormone synthesis in the gonads [47]. *FSHR* is highly expressed in ovarian granulosa cells; it

341   is a key gene involved in ovarian function and stimulated primarily by FSH to regulate follicle

342   growth and maturation, as well as estrogen production [48]. In our study, *FSHR* and

343   XLOC_021792 were highly expressed when FSH was the most secreted for ovulation (D16–

344   D03); therefore, a novel lncRNA, namely, XLOC_021792, could positively regulate *FSHR*

345   through a *cis*-acting relationship (Figure 6A). In addition, ovarian follicles have a characteristic

346   pattern of bioelectrical activity and ion transport mechanisms; they are also involved in a range

347   of oogenesis through Na^+, K^+, and Cl^- channel activation and ion transport [49, 50]. Among

348   the K^+ genes, *KCND2*, which acts as a steroid sensor and generates bioelectrical signals for

349   follicle production, and *KCNQ5* from the KCNQ family, which is an important substance in

350   ion channels in hamster ovarian cells, were identified in our sample [51, 52]. Our results

351   showed that *KCND2* could be negatively regulated as a *cis*-acting relationship from novel

lncRNA XLOC_017111 and known lncRNA ENSSSCG00000050977; *KCNQ5* was positively

regulated as a *cis*-acting relationship from novel lncRNA XLOC_000342 and the known

lncRNA ENSSSCG00000050380 (Figure 6A). Since the period of the high KNCD2 expression

(D7–D15), which acts as a steroid sensor, was very similar to the period of progesterone

secretion in the corpus luteum, XLOC_017111 and ENSSSCG00000050977, which were

negatively regulated in the *cis*-acting relationship, would affect progesterone secretion.

Tissue-specific lncRNAs of the oviduct were obtained from the network constructed

through the green module (Figure 3C). BP terms and KEGG pathways related to cell

morphogenesis and cell development in oviductal tissues were identified from the DE *cis*-

acting genes of these lncRNAs (Figure 5B). Among the lncRNA and *cis*-acting gene pairs

involved in these functions, four pairs had significant expression patterns and correlations

(Figure 6B). In the porcine oviductal tissue, MAP kinase activity stimulates gene expression

and cell division; it also favors the formation of epithelial cells of the fallopian tubes and

prevents the entry of toxic materials or pathogens by controlling permeability via tight

junctions [53-55]. *ERBB2*, which is involved in both of these key terms and in epithelial cell

development and signaling [56], is negatively regulated in a *cis*-acting relationship by

ENSSSCG00000045111, a known lncRNA (Figure 6B). In the period of high *ERBB2*

expression (D04–D15), the follicle moves to the uterus through the oviduct after ovulation to

prepare for pregnancy. ENSSSCG00000045111 was likely involved in the formation of tubal

epithelial tissue during this period.

The tissue-specific lncRNAs of the endometrium were obtained from the network

constructed through the red module (Figure 3D). The main terms related to uterine development

for embryo implantation were identified from the DE *cis*-acting genes of these lncRNAs

(Figure 5C). Among the lncRNA and *cis*-acting gene pairs involved in these functions, four

pairs had significant expression patterns and correlations (Figure 6C). Retinol (vitamin A) and

377 retinol-binding protein (RBP) secreted into the endometrium were implicated in the

378 development of the porcine endometrium and embryonic formation. These RBPs participate in

379 the storage, metabolism, and transport of retinol to target cells and in uterine growth and

380 morphogenesis. RBP has four morphological categories that affect the endometrium in various

381 ways [57-59]. In our study, among RBPs, *RBP1* was positively correlated with XLOC_008338,

382 a novel lncRNA; in comparison with other tissues, when XLOC_008338 was not expressed in

383 the endometrium, the expression of *RBP1* was also suppressed (Figure 6C). The expression of

384 *RBP1* possibly increased for implantation at the time of ovulation (D03), but the expression of

385 *RBP1* likely decreased because implantation did not occur (D4–D21). At this time, *NMNAT3*

386 had a high positive correlation in the *cis*-acting relationship such as *RBP1* and XLOC_008338,

387 and it was affected by XLOC_008338. *NMNAT3* likely participated in endometrial

388 morphogenesis.

389

390 ***Regulation of the steroid hormone during the estrous cycle by lncRNA***

391   Tissue-integrated lncRNAs were obtained from the yellow module constructed

392 according to the correlation of hormone changes (Figure 3E). The genes correlated in the *cis*-

393 acting relationship with these lncRNAs in all tissues and estrous cycles were *CHST9*, *DECR2*,

394 *KLF6*, *KLF11*, *MYBL2*, and *PCDH19* (Figure 6D, Figure S7). The KLF family can be

395 expressed in tissues that respond to steroid hormones in relation to the action of the

396 progesterone receptor (PGR) and estrogen receptor (ESR) [60]. In the present study, *KLF6* and

397 *KLF11* were highly expressed when PGF2α was secreted for ovarian P4 inhibition in the

398 endometrium (D16–D21); thus, P4 was inhibited and E2 was highly expressed in th eovary

399 during secretion. *KLF6* was highly correlated with novel lncRNA XLOC_004128, and *KLF11*

400 was highly correlated with known lncRNA ENSSSCG00000040267; This high correlation

401 seemed to be affected by the *cis*-acting relationship with lncRNAs (Figure 6D). Therefore,

402 these lncRNAs were likely closely related to the secretion of PGF2α from the endometrium

403 and the secretion of E2 from the ovary. *MYBL2* showed a similar expression pattern in the

404 endometrium and an opposite expression pattern in the ovary. XLOC_016616 also showed an

405 expression pattern similar to that of *MYBL2*, and this expression pattern was possibly regulated

406 in the *cis*-relationship (Figure 6D). Therefore, XLOC_016616 could be a lncRNA that could

407 affect the secretion of PGF2α from the endometrium and the secretion of P4 from the ovary.

408

409 ***Trans-acting and complex transcriptional participation by lncRNA***

410   The *trans*-acting relationship between lncRNA and coding gene is as important and

411 diverse as the *cis*-acting relationship although it is difficult to verify compared with the *cis*-

412 acting relationship and vague in setting the standard [37]. Usually, the relationship between a

413 lncRNA and a *trans*-acting gene means that they interact even when they are in different

414 chromosomes [61]. In the present study, the core lncRNA was selected through co-expression

415 network construction (Figure 3B, 3D). Core lncRNAs were highly correlated with the other

416 main lncRNAs in the network present in different chromosomes (Figure S8). Two core

417 lncRNAs, namely, XLOC_000748 and ENSSSCG00000051124, are presented as *trans*-acting

418 lncRNAs. In addition, a coding gene in a *cis*-acting relationship could be affected not only by

419 one lncRNA but also by several lncRNAs. Conversely, one lncRNA may affect multiple genes

420 in a *cis*-acting relationship [37]. In the present study, XLOC_003255, XLOC_008338,

421 XLOC_037548, and other lncRNAs had this potential (Figure 6A-C). The principle that

422 lncRNA regulates a gene as a *trans*-acting factor and various transcriptional regulation methods

423 of lncRNA are complex and diverse. Consequently, a more complete reference, including the

424 results of this study, should be established to accurately determine how lncRNA plays these

425 roles, and in-depth research based on structural analysis should be performed.

Conclusions

In this study, lncRNA (novel lncRNA and known lncRNA) and mRNA expressed during the swine estrous cycle were discovered in three reproductive tissues of pigs, and their expression patterns were similar. Network analysis was performed to analyze the function of lncRNA according to its expression pattern, and *cis*-acting genes were searched to understand the interaction between lncRNA and mRNA. The main lncRNA and *cis*-acting gene significantly expressed according to the estrous cycle in a tissue-specific or tissue-integrated manner were found, and their functions were presented. The expression of these lncRNA and *cis*-acitng gene could be highly related to hormonal activities secreted by each tissue. In the ovary, XLOC_021792 likely regulated FSH secretion during the follicular phase; XLOC_01711, ENSSSCG00000050977, XLOC_000342, and ENSSSCG00000050380 possibly regulated P4 secretion during the luteal phase. ENSSSCG00000045111 controlled the oviductal morphogenesis for pregnancy preparation during the luteal phase, and XLOC_008338 modulated the uterine morphogenesis in the estrus phase. XLOC_004128 and ENSSSCG00000040267 likely inhibited P4 secretion and activated E2 secretion in the ovary during the luteal phase. They were also related to the secretion of PGF2α from the endometrium during the proestrus period. XLOC_016616 was also presented to be a similar lncRNA. These results revealed the possible lncRNAs and their functions that have not been identified in porcine reproductive tissues according to the estrus cycle. Furthermore, this study could help elucidate the activities and interactions of reproductive tissues that were difficult to understand only when mRNA was used as a reference. This study also provided a basis for further research on the specific mechanism by which lncRNA regulates mRNA according to the structure and location of a given lncRNA sequence.

453 **Data availability**

454 All raw RNA-seq data were deposited at the NCBI Gene Expression Omnibus

455 (https://www.ncbi.nlm.nih.gov/geo/) under the accession number GSE108570.

456

462 **Conflict of interest statement**

463 The authors declare that they have no conflict of interest.

Literature cited

1.   Revelle, T.J. and O. Robison, An explanation for the low heritability of litter size in swine. Journal of Animal Science, 1973. 37(3): p. 668-675.

2.   Sharpe, R.M. and S. Franks, Environment, lifestyle and infertility—an inter-generational issue. Nature Medicine, 2002. 8(10): p. S33-S40.

3.   Cole, D., Nutritional strategies to optimize reproduction in pigs. Journal of Reproduction and Fertility, 1990(Supplement No. 40): p. 67-82.

4.   Li, P.-H., et al., Progress in the physiological and genetic mechanisms underlying the high prolificacy of the Erhualian pig. Yi Chuan= Hereditas, 2017. 39(11): p. 1016-1024.

5.   Zhang, F., et al., Changes in Ovary Transcriptome and Alternative splicing at estrus from Xiang pigs with Large and Small Litter Size. bioRxiv, 2019: p. 547810.

6.   Kim, J.-M., et al., Integrated transcriptomes throughout swine oestrous cycle reveal dynamic changes in reproductive tissues interacting networks. Scientific reports, 2018. 8(1): p. 1-14.

7.   Liu, Y., et al., Systematic analysis of Long non-coding RNAs and mRNAs in the ovaries of Duroc pigs during different follicular stages using RNA sequencing. International journal of molecular sciences, 2018. 19(6): p. 1722.

8.   Ross, J.W., et al., Activation of the transcription factor, nuclear factor kappa-B, during the estrous cycle and early pregnancy in the pig. Reproductive Biology and Endocrinology, 2010. 8(1): p. 1-17.

9.   Soede, N., P. Langendijk, and B. Kemp, Reproductive cycles in pigs. Animal reproduction science, 2011. 124(3-4): p. 251-258.

10. Edson, M.A., A.K. Nagaraja, and M.M. Matzuk, The mammalian ovary from genesis to revelation. Endocrine reviews, 2009. 30(6): p. 624-712.

11. Noguchi, M., et al., Peripheral concentrations of inhibin A, ovarian steroids, and gonadotropins associated with follicular development throughout the estrous cycle of the sow. Reproduction, 2010. 139(1): p. 153.

12. Leese, H., The formation and function of oviduct fluid. Reproduction, 1988. 82(2): p. 843-856.

13. Akison, L.K., et al., Progesterone receptor-dependent regulation of genes in the oviducts of female mice. Physiological Genomics, 2014. 46(16): p. 583-592.

14. Wang, Y., et al., Analyses of long non-coding RNA and mRNA profiling using RNA sequencing during the

493   pre-implantation phases in pig endometrium. Scientific reports, 2016. 6(1): p. 1-11.

494   15. Hunter, R., B. Cook, and N. Poyser, Regulation of oviduct function in pigs by local transfer of ovarian
495   steroids and prostaglandins: a mechanism to influence sperm transport. European Journal of Obstetrics &
496   Gynecology and Reproductive Biology, 1983. 14(4): p. 225-232.

497   16. Park, Y., et al., Time Series Ovarian Transcriptome Analyses of the Porcine Estrous Cycle Reveals Gene
498   Expression Changes during Steroid Metabolism and Corpus Luteum Development. Animals, 2022. 12(3): p.
499   376.

500   17. Jang, M.-J., et al., Integrated multiple transcriptomes in oviductal tissue across the porcine estrous cycle
501   reveal functional roles in oocyte maturation and transport. Journal of animal science, 2022. 100(2): p.
502   skab364.

503   18. Ma, L., V.B. Bajic, and Z. Zhang, On the classification of long non-coding RNAs. RNA biology, 2013. 10(6):
504   p. 924-933.

505   19. Leung, A., et al., Novel long noncoding RNAs are regulated by angiotensin II in vascular smooth muscle
506   cells. Circulation research, 2013. 113(3): p. 266-278.

507   20. Li, B.J., et al., Genome-wide identification and differentially expression analysis of lncRNAs in tilapia. BMC
508   genomics, 2018. 19(1): p. 1-12.

509   21. Chen, L., et al., Transcriptome analysis suggests the roles of long intergenic non-coding RNAs in the growth
510   performance of weaned piglets. Frontiers in genetics, 2019. 10: p. 196.

511   22. Sun, Q., Q. Hao, and K.V. Prasanth, Nuclear long noncoding RNAs: key regulators of gene expression.
512   Trends in Genetics, 2018. 34(2): p. 142-157.

513   23. Statello, L., et al., Gene regulation by long non-coding RNAs and its biological functions. Nature reviews
514   Molecular cell biology, 2021. 22(2): p. 96-118.

515   24. Kosinska-Selbi, B., M. Mielczarek, and J. Szyda, Long non-coding RNA in livestock. animal, 2020. 14(10):
516   p. 2003-2013.

517   25. Gong, Y., et al., lncRNA-screen: an interactive platform for computationally screening long non-coding
518   RNAs in large genomics datasets. BMC genomics, 2017. 18(1): p. 1-18.

519   26. Huarte, M., The emerging role of lncRNAs in cancer. Nature medicine, 2015. 21(11): p. 1253-1261.

520   27. Jiang, P., et al., Characterization of lncRNAs involved in cold acclimation of zebrafish ZF4 cells. PloS one,
521   2018. 13(4): p. e0195468.

522   28. Li, Z., et al., Tumor-derived exosomal lnc-Sox2ot promotes EMT and stemness by acting as a ceRNA in
523   pancreatic ductal adenocarcinoma. Oncogene, 2018. 37(28): p. 3822-3838.

524   29. Jiang, L., et al., Identification and expression analysis of lncRNA in seven organs of Rhinopithecus roxellana.
525   Functional & Integrative Genomics, 2021. 21(5): p. 543-555.

526   30. Zhang, Y., et al., New insight into long non-coding RNAs associated with bone metastasis of breast cancer
527   based on an integrated analysis. Cancer cell international, 2021. 21(1): p. 1-17.

528   31. Wang, Y., et al., mRNA/lncRNA expression patterns and the function of fibrinogen-like protein 2 in Meishan
529   pig endometrium during the preimplantation phases. Molecular Reproduction and Development, 2019. 86(4):
530   p. 354-369.

531   32. Subramanian, I., et al., Multi-omics data integration, interpretation, and its application. Bioinformatics and
532   biology insights, 2020. 14: p. 1177932219899051.

533   33. Quirós, P.M., et al., Multi-omics analysis identifies ATF4 as a key regulator of the mitochondrial stress
534   response in mammals. Journal of Cell Biology, 2017. 216(7): p. 2027-2045.

535   34. Zapparoli, E., et al., Comprehensive multi-omics analysis uncovers a group of TGF-β-regulated genes among
536   lncRNA EPR direct transcriptional targets. Nucleic acids research, 2020. 48(16): p. 9053-9066.

537   35. Yanai, I., et al., Genome-wide midrange transcription profiles reveal expression level relationships in human
538   tissue specification. Bioinformatics, 2005. 21(5): p. 650-659.

539   36. Knox, R., et al., Plasma gonadotropins and ovarian hormones during the estrous cycle in high compared to
540   low ovulation rate gilts. Journal of animal science, 2003. 81(1): p. 249-260.

541   37. Gil, N. and I. Ulitsky, Regulation of gene expression by cis-acting long non-coding RNAs. Nature Reviews
542   Genetics, 2020. 21(2): p. 102-117.

543   38. Kumar, H., et al., Transcriptome analysis to identify long non coding RNA (lncRNA) and characterize their
544   functional role in back fat tissue of pig. Gene, 2019. 703: p. 71-82.

545   39. Gong, Y., et al., Integrated Analysis of lncRNA and mRNA in Subcutaneous Adipose Tissue of Ningxiang
546   Pig. Biology, 2021. 10(8): p. 726.

547   40. Song, F., et al., Long noncoding RNA and mRNA expression profiles following igf3 knockdown in common
548   carp, Cyprinus carpio. Scientific data, 2019. 6(1): p. 1-8.

549   41. Nakamura, S., et al., Relationship between sonographic endometrial thickness and progestin-induced
550   withdrawal bleeding. Obstetrics & Gynecology, 1996. 87(5): p. 722-725.

551   42. Skarzynski, D., M. Bogacki, and J. Kotwica, Involvement of ovarian steroids in basal and oxytocin-
552   stimulated prostaglandin (PG) F2α secretion by the bovine endometrium in vitro. Theriogenology, 1999.
553   52(3): p. 385-397.

554   43. Zhang, Z. and D. Davis, Prostaglandin E and F2α secretion by glandular and stromal cellsof the pig
555   endometrium in vitro: Effects of estradiol-17β, progesterone, and day of pregnancy. Prostaglandins, 1991.
556   42(2): p. 151-162.

557   44. SIMMEN, R.C., et al., Hormonal regulation of insulin-like growth factor gene expression in pig uterus.
558   Endocrinology, 1990. 127(5): p. 2166-2174.

559   45. Fortín, S., B.L. Sayre, and G.S. Lewis, Does exogenous progestogen alter the relationships among PGF2α,
560   13, 14-dihydro-15-keto-PGF2α, progesterone, and estrogens in ovarian-intact ewes around the time of
561   luteolysis? Prostaglandins, 1994. 47(3): p. 171-187.

562   46. McCracken, J., M. Glew, and R. Scaramuzzp, Corpus luteum regression induced by prostaglandin F2α. The
563   Journal of Clinical Endocrinology & Metabolism, 1970. 30(4): p. 544-546.

564   47. Mu, R., et al., Transcriptome analysis of ovary tissues from low-and high-yielding Changshun green-shell
565   laying hens. BMC genomics, 2021. 22(1): p. 1-11.

566   48. Zhang, Y., et al., Effect of human amniotic epithelial cells on ovarian function, fertility and ovarian reserve
567   in primary ovarian insufficiency rats and analysis of underlying mechanisms by mRNA sequencing.
568   American Journal of Translational Research, 2020. 12(7): p. 3234.

569   49. Krüger, J. and J. Bohrmann, Bioelectric patterning during oogenesis: stage-specific distribution of membrane
570   potentials, intracellular pH and ion-transport mechanisms in Drosophila ovarian follicles. BMC
571   developmental biology, 2015. 15(1): p. 1-13.

572   50. Fazelkhah, A., et al., Quantitative model for ion transport and cytoplasm conductivity of chinese hamster
573   ovary cells. Scientific reports, 2018. 8(1): p. 1-12.

574   51. Mayerhofer, A. and L. Kunz, Ion channels of primate ovarian endocrine cells: identification and functional
575   significance. Expert review of endocrinology & metabolism, 2006. 1(4): p. 549-555.

576   52. Gamper, N., J.D. Stockand, and M.S. Shapiro, The use of Chinese hamster ovary (CHO) cells in the study of
577   ion channels. Journal of pharmacological and toxicological methods, 2005. 51(3): p. 177-185.

578   53. Wollenhaupt, K., et al., Effects of ovarian steroids and epidermal growth factor (EGF) on expression and
579   bioactivation of specific regulators of transcription and translation in oviductal tissue in pigs.
580   REPRODUCTION-CAMBRIDGE-, 2002. 123(1): p. 87-96.

581   54. Ariyadi, B., N. Isobe, and Y. Yoshimura, Expression of tight junction molecule "claudins" in the lower
582   oviductal segments and their changes with egg-laying phase and gonadal steroid stimulation in hens.
583   Theriogenology, 2013. 79(2): p. 211-218.

584 55. Chen, S., R. Einspanier, and J. Schoen, Transepithelial electrical resistance (TEER): a functional parameter
585   to monitor the quality of oviduct epithelial cells cultured on filter supports. Histochemistry and cell biology,
586   2015. 144(5): p. 509-515.

587 56. Lim, C.-H., et al., Estrogen Regulates ERRFI1 Expression during Development of the Chicken Oviduct.
588   Regular Conference and Presentation of the Korean Poultry Society, 2011: p. 121-122.

589 57. Schweigert, F.J., et al., Distribution of vitamin A, retinol-binding protein, cellular retinoic acid-binding
590   protein I, and retinoid X receptor β in the porcine uterus during early gestation. Biology of reproduction,
591   1999. 61(4): p. 906-911.

592 58. Ma, X., et al., Genome-wide association analysis reveals genomic regions on Chromosome 13 affecting litter
593   size and candidate genes for uterine horn length in Erhualian pigs. Animal, 2018. 12(12): p. 2453-2461.

594 59. Chen, X., et al., Differential gene expression in uterine endometrium during implantation in pigs. Biology of
595   reproduction, 2015. 92(2): p. 52, 1-14.

596 60. Heard, M.E., et al., Krüppel-like factor 13 deficiency in uterine endometrial cells contributes to defective
597   steroid hormone receptor signaling but not lesion establishment in a mouse model of endometriosis. Biology
598   of reproduction, 2015. 92(6): p. 140, 1-9.

599 61. Elling, R., et al., Genetic models reveal cis and trans immune-regulatory activities for lincRNA-Cox2. Cell
600   reports, 2018. 25(6): p. 1511-1524. e6.

601

FIGURES LEGENDS

603
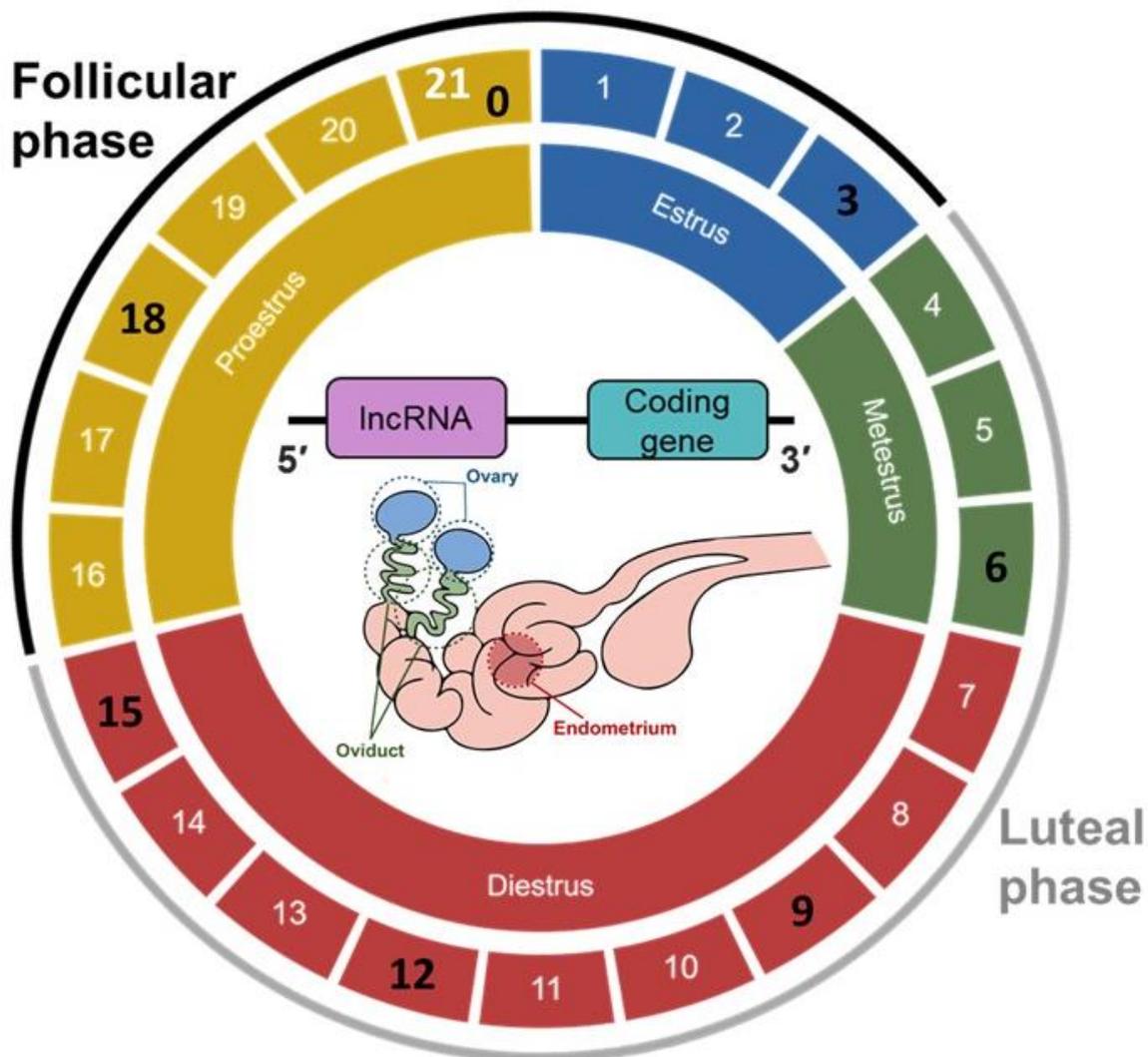
Figure 1. Overview of three reproductive tissue transcriptomes (lncRNA, coding gene) throughout the estrous cycle. The number of samples (n=3) in swine reproductive tissue at seven time points (D00, D03, D06, D09, D12, D15, and D18) on the stages of the estrous cycle.

607
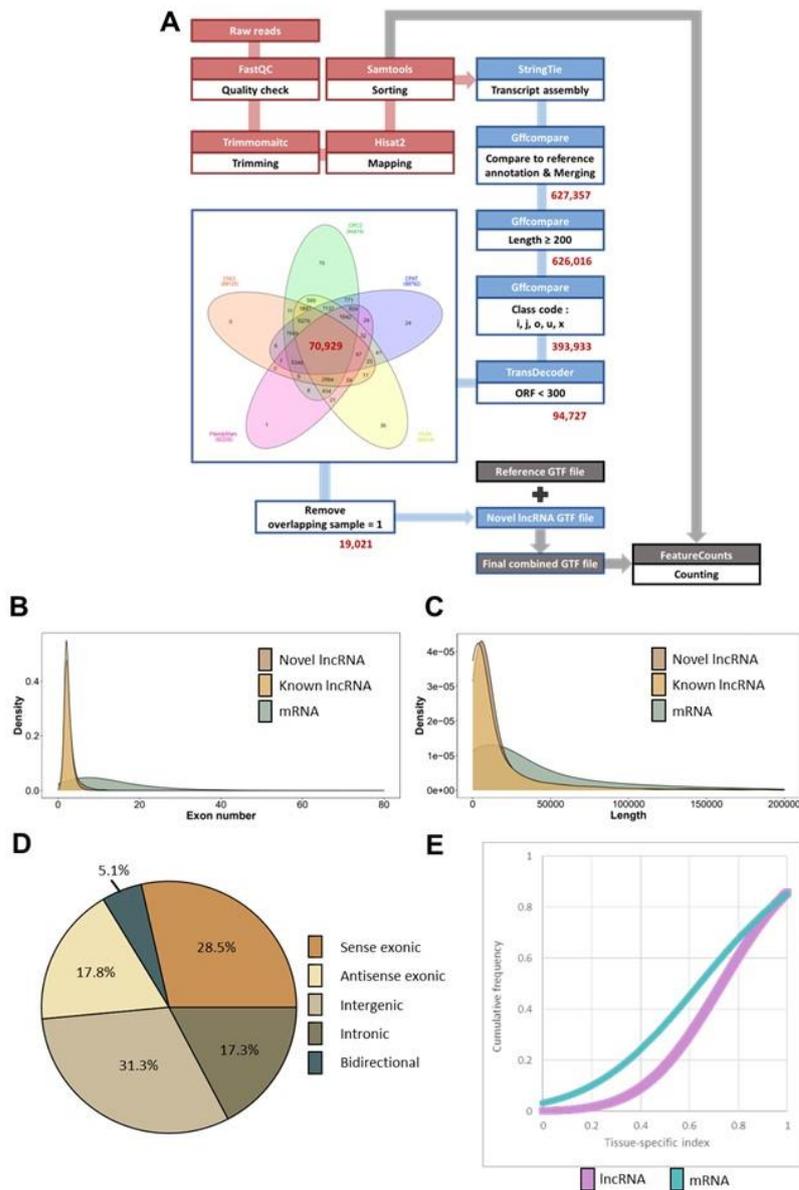
Figure 2. Acquisition and genomic characterization of the novel lncRNA. (A) Filtering and number of novel lncRNA. (B) Comparison of the distribution of the exon number between lncRNAs (novel lncRNAs and known lncRNAs) and mRNAs. (C) Comparison of the distribution of the transcript length between lncRNAs (novel lncRNAs and known lncRNAs) and mRNAs. (D) Classification of novel lncRNAs. Percentage of exonic, intergenic, intronic, and bidirectional regions. (E) Comparison of the tissue-specific index (TSI) of lncRNA and mRNA. The cumulative distribution of TSI of lncRNAs (novel lncRNAs and known lncRNAs) and mRNAs.
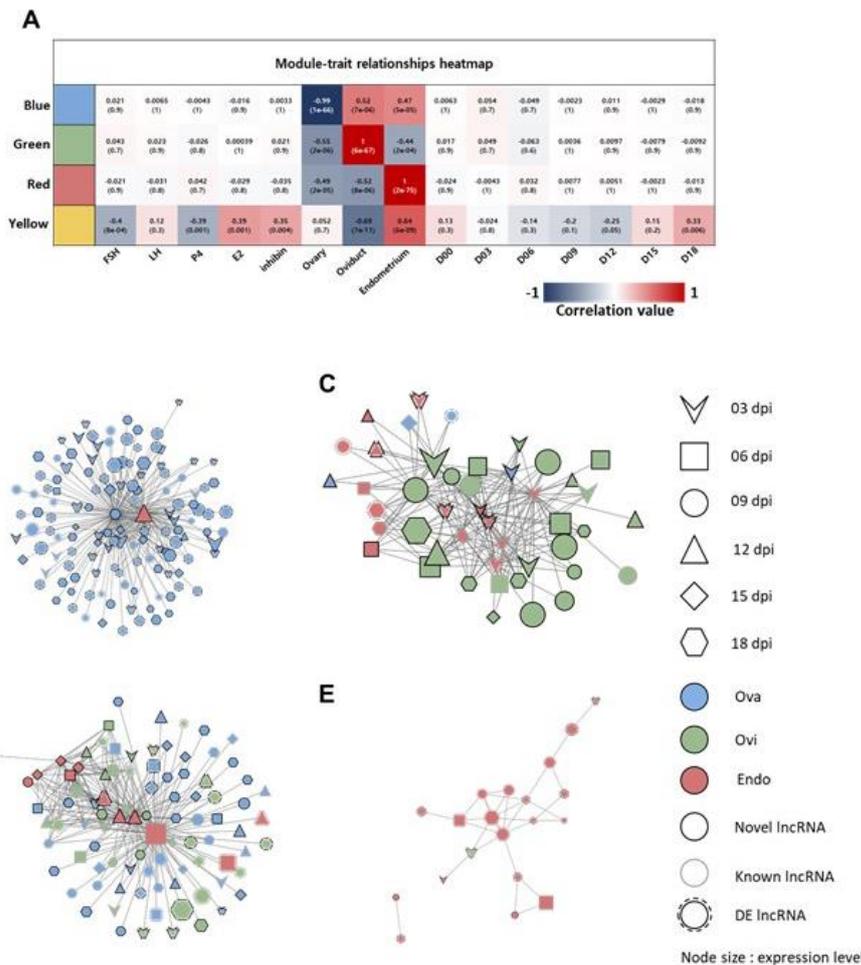
Figure 3. Network analysis of lncRNA based on the heatmap of four module–trait relationships. Node color indicates three tissues, node size corresponds to the expression level, and node shape refers to the six time points (D03: V shape; D06: rectangle; D09: ellipse; D12: triangle; D15: diamond; D18: hexagon). The border of the node indicates the types of lncRNA (novel lncRNA: black line; known lncRNA: gray line; DE lncRNA: parallel line). The red star refers to the core lncRNA. (A) Heatmap of four module–trait relationships of lncRNA according to hormones, tissues (ovary, oviduct, endometrium), and days (D00, D03, D06, D09, D12, D15, D18). (B) Correlation network of lncRNAs in the blue module. The lncRNA marked with a red star is XLOC_000748. (C) Correlation network of lncRNAs in the green module. (D) Correlation network of lncRNAs in the red module. The lncRNA marked with a red star is ENSSSCG00000051124. (E) Correlation network of lncRNAs in the yellow module.

629
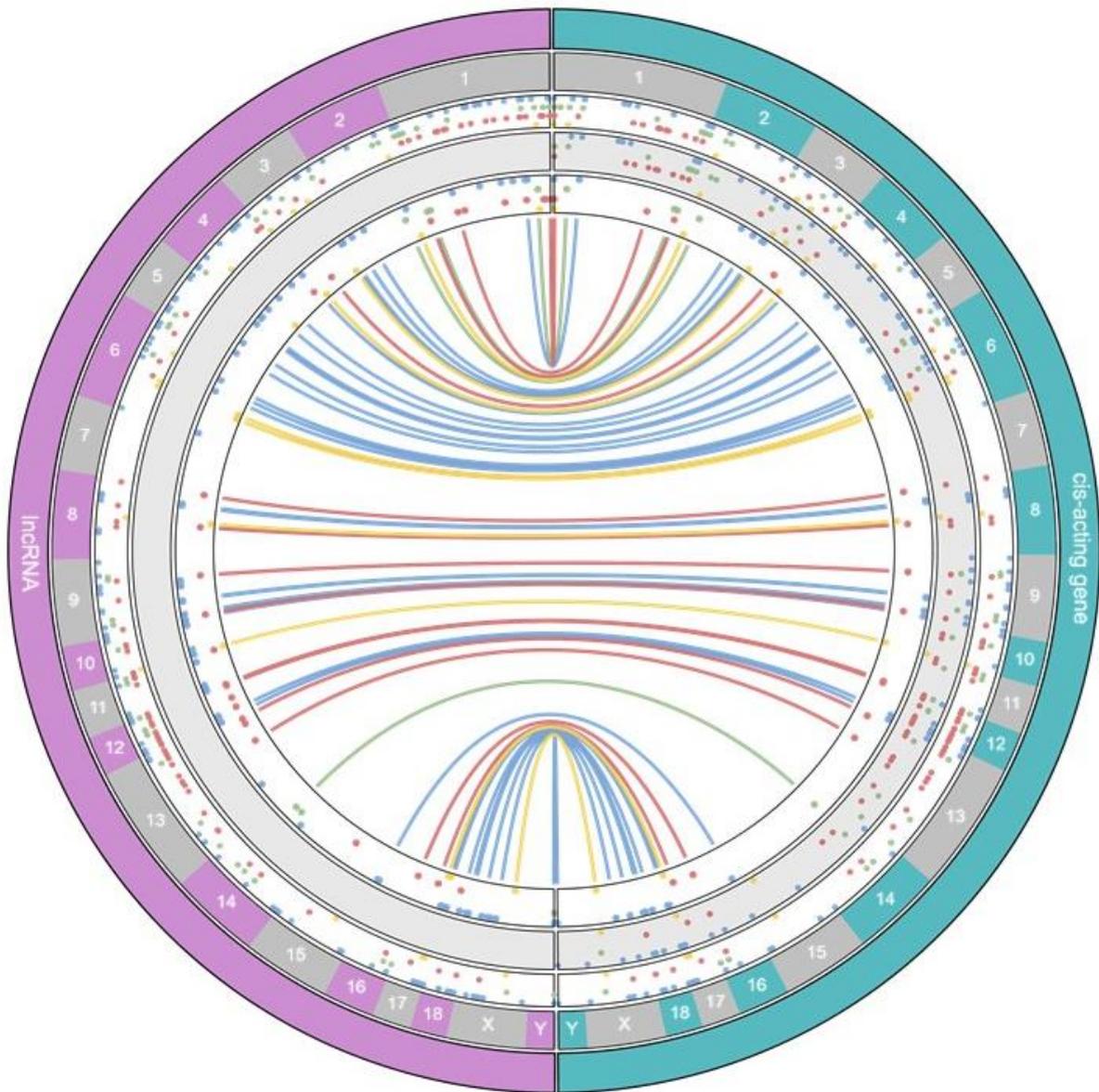
Figure 4. Distribution of lncRNA and the *cis*-acting gene for each network in different chromosomes. The outer layer of the lncRNA category indicates the lncRNA included in the network for each module, and the inner layer contains only DE lncRNAs among them. The outer layer of the *cis*-acting gene category refers to the *cis*-acting gene of lncRNAs included in the network for each module, the middle layer contains only DE *cis*-acting gene from the outer layer, and the innermost layer contains only the *cis*-acting gene of DE lncRNA in the middle layer. The innermost circle shows the linkage between the DE lncRNA of each network and their DE *cis*-acting gene.
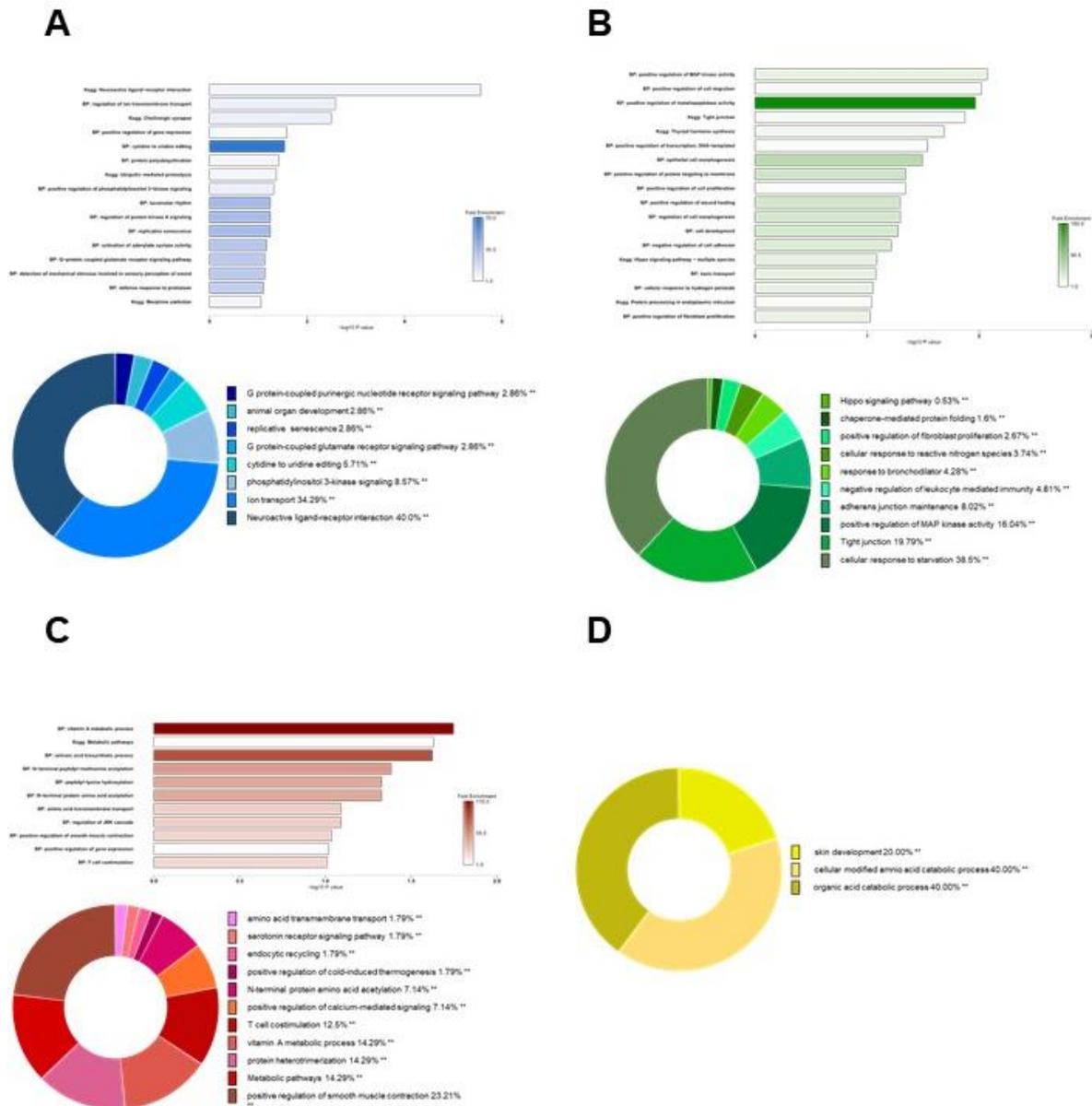
**Figure 5. Visualization of the functional analyses of DE *cis*-acting gene of lncRNAs included in the network for each module.** Bar graph of biological process (BP) and Kyoto Encyclopedia of Genes and Genomes (KEGG) pathways using DAVID analysis. Pie chart of BP term and KEGG pathways via Cytoscape (** $p < 0.05$). (A) Bar graph and pie chart of the correlation network of lncRNAs in the blue, (B) green, and (C) red modules. (D) Pie chart of the correlation network of lncRNAs in the yellow module.
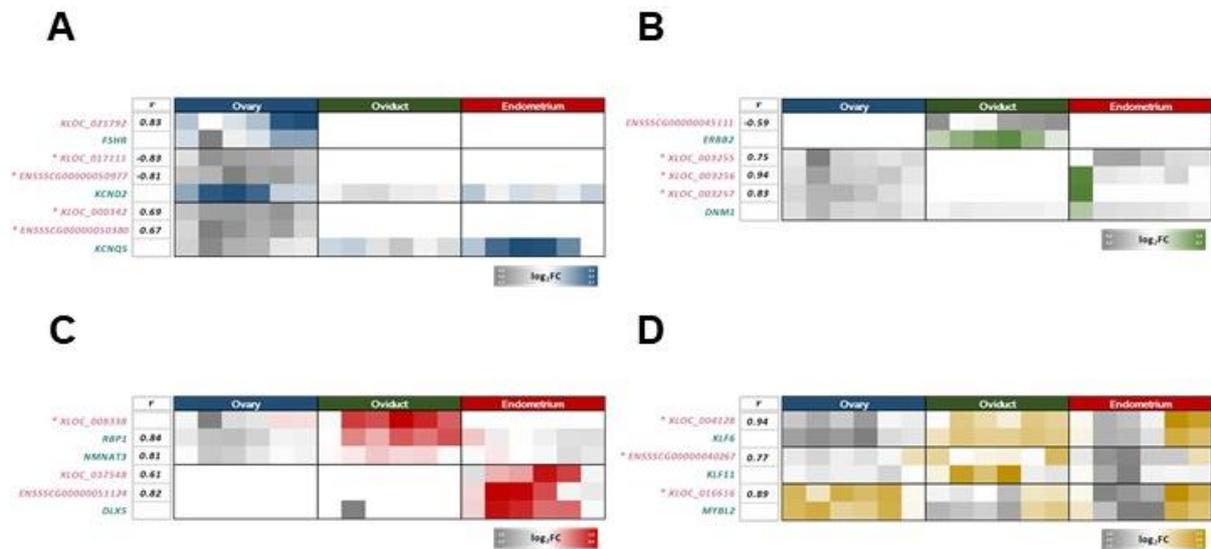
Figure 6. Correlation heatmap of the main lncRNA and *cis*-acting gene. Correlation coefficients (*r*) were calculated as log$_2$FC values. Log$_2$FC of D03, D06, D09, D12, D15, and D18 in order from the first column to the last column of each tissue category. LncRNAs marked with an asterisk (*) indicate DElncRNAs. (A) Correlation heatmap of the main lncRNA and *cis*-acting gene of the network from the blue, (B) green, (C) red, and (D) yellow modules.